Nonlinear Maneuver Regulation for Reduced-G Atmospheric Flight

Juan-Pablo Afman[1], Eric Feron[1], John Hauser[2]

***Abstract*— In order to address the need for an autonomous reduced-gravity enabling platform, a novel flight-control architecture has been formulated. The chosen control law employs a chain of three integrators, taking advantage of the internal model principle to counteract the nonlinear aerodynamic forces impeding the vehicle's constant acceleration during vertical flight. Due to the nonlinear feedback arising from the aerodynamic disturbance, stability is studied via the formulation of the closed-loop transverse dynamics and the application of the circle criterion to prove their stability.**

MOTIVATION

Enabling reliable reduced-gravity environments for relevant temporal intervals is the objective behind this work. A wide range of scientific disciplines employ reduced-gravity conditions as a tool to investigate phenomena of processes in the absence of Earth's gravitational field. These disciplines include life sciences as well as physical sciences. Although reduced-gravity research has proven itself useful for public benefit through breakthroughs in pharmaceutics, metallurgy, communications, electronics, and so on, foundations in automatic control for reliable unmanned parabolic flight have only recently been explored by the authors [1], [2]. Our prior work explored a conceptual vehicle as well as the controller architecture, leading to the first known relevant application of triple-integral control. Although this controller has been successfully implemented in a full nonlinear simulation of a multi-rotor with variable pitch actuation, and further validated through experimental flight, formal guarantees regarding the stability of the vertical-flight maneuver have been left in question. This work focuses on providing stability guarantees for the free-fall maneuver under this novel triple-integral control law subject to the nonlinear feedback disturbance (drag) via the formation of the transverse dynamics and an application of the circle criterion. Although the concepts presented in this paper are illustrated with a variable-pitch multi-rotor, they are applicable to a much broader class of vehicles, including fixed-wing aircraft and appropriately designed roller coasters that may be used to generate reduced-gravity environments.

This paper is organized as follows. The section on vertical flight reminds the reader of the nonlinear dynamics of objects in atmospheric flight. The next two sections on maneuver feasibility and linear regulation and disturbance rejection refer to the triple integrator controller structure presented in our previous paper [1]. The sections devoted to nonlinear maneuver regulation and transverse dynamics constitute our core contribution of this paper and develop the nonlinear stability properties of the closed-loop system.

[1]Juan-Pablo Afman and Eric Feron are with the Department of Aerospace Engineering at the Georgia Institute of Technology, Atlanta, GA 30332.

[2]John Hauser is with the Department of Electrical, Computer, & Energy Engineering, University of Colorado Boulder, Boulder, CO 80309.

VERTICAL FLIGHT

The vertical velocity of a flying vehicle, with $v > 0$ when descending, evolves according to

$$\dot{v} = g - bv|v| + a_p$$

where $-bv|v|$ models the acceleration due to aerodynamic drag (acting to retard the motion), g is the acceleration of (earth) gravity, and a_p is the thrusting acceleration. Clearly, the constant desired acceleration a_d could be achieved using

$$a_p = a_d - g + bv|v|$$

provided v is perfectly measured, b is known, and a_p is directly controlled—impossible conditions in practice.

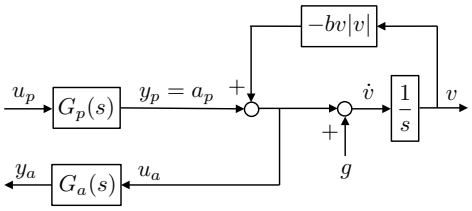

Fig. 1. Vertical Flight Vehicle model

Figure 1 provides us with a more realistic model for a vehicle in vertical flight, where the thrusting acceleration a_p is produced by a motor-propeller-servo system and the (non-gravity) acceleration $a_p - bv|v|$ (as filtered by the vehicle, accelerometer, and mounting structures) is measured by an accelerometer system. Here the actuator and sensing systems are taken to be stable and minimum phase LTI systems, $G_p(s) = c_p^T(sI - A_p)^{-1}b_p$ and $G_a(s) = c_a^T(sI - A_a)^{-1}b_a$, with unit DC gain, $G_p(0) = 1 = G_a(0)$. While the available thrusting acceleration will certainly saturate, within operating limits, its dynamics is well modeled as a linear time-invariant system.

MANEUVER FEASIBILITY

We are interested in enabling a *free-fall* type maneuver in which the vehicle begins at a given altitude and accelerates downward with a constant desired acceleration $a_d > 0$, resulting in a linearly increasing velocity $v = a_d t \geq 0$, automatically compensating for the naturally occurring drag force/acceleration. When $a_d = 1\,g$, the goal is indeed free fall. In some cases, such as when simulating gravity on Mars, we merely choose to accelerate downward at a desired acceleration less than one g. For the time being, we will consider the falling scenario, leaving the interesting *toss*

and fall case for a future discussion. To understand what is needed to perform such a maneuver, consider a trajectory with $\tilde{v}(t) = a_d t$ so that the output of the propeller/servo system needs to be $\tilde{y}_p(t) = ba_d^2 t^2 + a_d - g$, as shown in Figure 2.

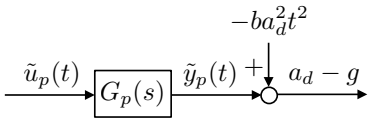

Fig. 2. A desired falling trajectory/maneuver

The actuated propeller system $G_p(s)$ is capable of producing this output, as the following simple *inversion* result shows.

Lemma 1: Let $G(s) = c^T(sI - A)^{-1}b$ be stable with $G(0) = 1$. Then every polynomial output $y(t) = y_0 + y_1 t + \cdots + y_k t^k/k!$ can be produced with a corresponding polynomial input $u(t) = u_0 + u_1 t + \cdots + u_k t^k/k!$ and state $x(t) = x_0 + x_1 t + \cdots + x_k t^k/k!$.

Proof: The claim leads to a simple set of solvable linear equations. To get a sense of this, useful in our setting, consider $y(t) = t^2/2$. We have

$$\begin{aligned} t^2/2 &= c^T(x_0 + x_1 t + x_2 t^2/2) \\ x_1 + x_2 t &= A(x_0 + x_1 t + x_2 t^2/2) + b(u_0 + u_1 t + u_2 t^2/2) \end{aligned}$$

giving rise to the set of equations

$$\begin{array}{llll} 1 = c^T x_2 & & 0 = A x_2 + b u_2 \\ 0 = c^T x_1 & & x_2 = A x_1 + b u_1 \\ 0 = c^T x_0 & & x_1 = A x_0 + b u_0 \end{array}$$

Since A is invertible (by stability) and $-c^T A^{-1} b = 1$ (no zero at $s = 0$), the solution is easily seen to be

$$\begin{array}{llll} u_2 = 1 & & x_2 = -A^{-1}b \\ u_1 = c^T A^{-2} b & & x_1 = -A^{-2}b - (c^T A^{-2} b) A^{-1} b \\ u_0 = c^T A^{-3} b & & x_0 = -A^{-3}b - (c^T A^{-2} b) A^{-2} b \\ \quad + (c^T A^{-2} b)^2 & & \quad - (c^T A^{-3} b + (c^T A^{-2} b)^2) A^{-1} b \end{array}$$

Monomials of any order may be solved in a similar manner, with polynomials following by linearity. ∎

The state and input trajectories corresponding to this (quadratic in t) output are thus also quadratic and, by linearity, of the form

$$\begin{aligned} \tilde{x}_p(t) &= ba_d^2(x_0 + x_1 t + x_2 t^2/2) + (a_d - g)x_{00} \\ \tilde{u}_p(t) &= ba_d^2(u_0 + u_1 t + u_2 t^2/2) + (a_d - g) \end{aligned}$$

where the coefficients of the quadratic polynomials are those found in the proof of the Inversion Lemma (with A_p, b_p, c_p) and x_{00} is the equilibrium state of $G_p(s)$ with a constant input of 1.

Now, the required quadratic input $\tilde{u}_p(t)$ for the drag compensated maneuver should be provided by the output $\tilde{y}_c(t)$ of our (to be designed) controller $C(s)$ with *zero* input $\tilde{u}_c(t) \equiv 0$. This can be accomplished using a chain of three integrators as shown in Figure 3, providing constant (or step), linear (or ramp), and quadratic components in its output under zero input conditions.

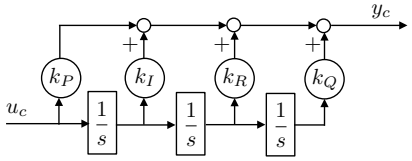

Fig. 3. Realization of the PIRQ control system

The transfer function of this *PIRQ* (Proportional-Integral-Ramp-Quadratic) controller is

$$C(s) = \frac{k_P s^3 + k_I s^2 + k_R s + k_Q}{s^3}$$

with state space realization

$$\left[\begin{array}{c|c} A_c & b_c \\ \hline c_c^T & d_c \end{array}\right] = \left[\begin{array}{cccc} 0 & 1 & 0 & 0 \\ 0 & 0 & 1 & 0 \\ 0 & 0 & 0 & 1 \\ \hline k_Q & k_R & k_I & k_P \end{array}\right]$$

and where the PIRQ coefficients are all positive (and subject to some further [stability] conditions below).

With zero input, the controller state for the falling maneuver will have the form

$$\tilde{x}_c(t) = \left[\begin{array}{c} q_0 + r_0 t + s_0 t^2/2 \\ r_0 + s_0 t \\ s_0 \end{array}\right]$$

so that, equating the controller output with the maneuver actuator input, we find that the required controller initial condition is

$$\tilde{x}_c(0) = \left[\begin{array}{c} q_0 \\ r_0 \\ s_0 \end{array}\right] = \left[\begin{array}{c} \frac{1}{k_Q}\left(u_{0p} - \frac{k_R}{k_Q}u_{1p} + \frac{k_R^2 - k_I k_Q}{k_Q^2}u_{2p}\right) \\ \frac{1}{k_Q}\left(u_{1p} - \frac{k_R}{k_Q}u_{2p}\right) \\ \frac{1}{k_Q}u_{2p} \end{array}\right]$$

where u_{0p}, u_{1p}, u_{2p} are the coeffficients of $\tilde{u}_p(t)$ above so that, e.g., $u_{1p} = ba_d^2 u_1$. This shows that the controller and actuator are capable of producing the signals needed to compensate the drag during an ideal maneuver.

Linear Regulation and Disturbance Rejection

In fact, this control system can be used to determine, in a feedback manner, the internal trajectory leading to asymptotic rejection of the *idealized disturbance* $-ba_d^2 t^2$, illustrated in Figure 4, without knowledge of b (or even a_d). Here $1/s^3$ provides an *internal model* for the (idealized maneuver drag) disturbance t^2. Asymptotic disturbance rejection is obtained for the linear feedback system in Figure 4 provided that $C(s)$ stabilizes the feedback loop. This is possible when $G_p(s)$ and $G_a(s)$ are (exponentially) stable and minimum phase. This is accomplished by choosing the (open left half plane) location of the zeros of

$$s^3 + \frac{k_I}{k_P}s^2 + \frac{k_R}{k_P}s + \frac{k_Q}{k_P}$$

and the overall gain k_P to bring the three compensator poles (at 0) into the open left half plane without moving the

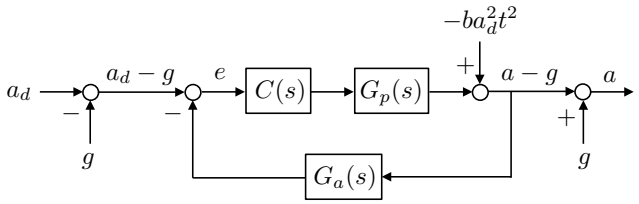

Fig. 4. PIRQ controller for rejecting idealized drag acceleration disturbance

stable poles of $G_s(s)$ and $G_a(s)$ into the right half plane. With closed loop stability, the actuator and controller states will converge $x_p(t) \to \tilde{x}_p(t)$ and $x_c(t) \to \tilde{x}_c(t)$ as $t \to \infty$ and the sensor state will converge to its constant value, $x_a(t) \to \tilde{x}_a = -A_a^{-1} b_a (a_d - g)$.

Nonlinear Maneuver Regulation

As noted, the feedback system in Figure 4 is idealized in the sense that the drag disturbance is modeled as a *function of time* when, in reality, this disturbance depends on the velocity state v as shown in Figure 5. The dynamics of this *nonlinear*

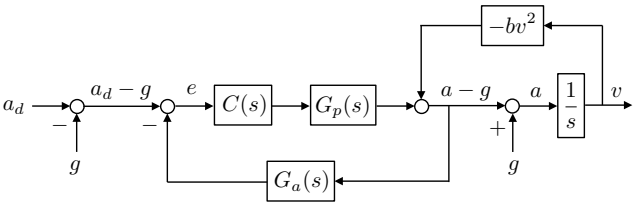

Fig. 5. Vertical Flight Vehicle with Maneuver Regulation

system is given by

$$\dot{v} = c_p^T x_p - bv^2 + g \tag{1}$$

$$\begin{bmatrix} \dot{x}_p \\ \dot{x}_c \\ \dot{x}_a \end{bmatrix} = \begin{bmatrix} A_p & b_p c_c^T & -b_p d_c c_a^T \\ 0 & A_c & -b_c c_a^T \\ b_a c_p^T & 0 & A_a \end{bmatrix} \begin{bmatrix} x_p \\ x_c \\ x_a \end{bmatrix} + \begin{bmatrix} b_p d_c \\ b_c \\ 0 \end{bmatrix} (a_d - g) + \begin{bmatrix} 0 \\ 0 \\ -b_a b v^2 \end{bmatrix} \tag{2}$$

and, by construction, we see that

$$(v, x_p, x_c, x_a)(t) = (a_d t, \tilde{x}_p(t), \tilde{x}_c(t), \tilde{x}_a)$$

is a trajectory of the system. The state space curve traced out by this trajectory is our desired *maneuver*. By maneuver, we mean an invariant curve of the dynamics in the state space.

While the linear feedback loop has been stabilized by a chosen PIRQ controller, the injection of the nonlinear feedback $-bv^2$ into the loop may cause trouble.

Indeed, what kind of stability might we expect for the system depicted in Figure 5? Clearly, we are hoping that the velocity increases according to $\dot{v} = a_d$ so it doesn't seem like we are looking for stability for v, though perhaps we would like to somehow regulate $\dot{v}$ to the desired acceleration a_d. Also, note that we cannot accelerate for too long before we exceed the operating envelope, limited by the speed of sound, propulsive actuator limits and the height of the maneuvering airspace.

What we would like is to make the desired maneuver *exponentially attractive*. Again, by maneuver, we mean an invariant curve in the (combined) state space with state (v, x_p, x_c, x_a). When discussing maneuvers, it is useful to keep in mind the case of a periodic orbit maneuver and the notion of orbital stability. [3]–[6]

Above, for a given desired velocity trajectory $\tilde{v}(t) = a_d t$ with fixed $a_d > 0$, we were able to *construct* the corresponding state trajectory $(\tilde{x}_p(t), \tilde{x}_c(t), \tilde{x}_a)$ for $t \geq 0$. This trajectory traces out a curve in (v, x_p, x_c, x_a) space and since $t \mapsto \tilde{v}(t) = a_d t$ is monotonically increasing (for $a_d > 0$), we may use its inverse $\bar{t}(v) = v/a_d$ to provide a parametrization of the *maneuver* by v. Indeed, defining $\bar{x}_p(v) = \tilde{x}_p(\bar{t}(v))$, $\bar{x}_c(v) = \tilde{x}_c(\bar{t}(v))$, and $\bar{x}_a = \tilde{x}_a$, we obtain the desired maneuver $(v, \bar{x}_p(v), \bar{x}_c(v), \bar{x}_a) = (v, \bar{x}(v))$, $v \geq 0$. We will use γ_{a_d} to refer to the maneuver corresponding to the desired acceleration a_d, although we will not explicitly label $\bar{x}_p(v)$, etc., with a_d. Note that γ_{a_d} is an invariant curve of the nonlinear feedback system described by (1), (2) and Figure 5.

Working from defining properties above, we see that the maneuver curves satisfy

$$c_p^T \bar{x}_p(v) = bv^2 + a_d - g \tag{3}$$

$$\bar{x}_p'(v)\, a_d = A_p \bar{x}_p(v) + b_p c_c^T \bar{x}_c(v) \tag{4}$$

$$\bar{x}_c'(v)\, a_d = A_c \bar{x}_c(v) \tag{5}$$

$$c_a^T \bar{x}_a = a_d - g \tag{6}$$

$$0 = A_a \bar{x}_a + b_a (a_d - g) \tag{7}$$

with $'$ being differentiation with respect to the argument v so that, e.g., $\bar{x}_p'(v) = (d/dv)\bar{x}_p(v)$.

Transverse Dynamics

In order to characterize the nature of the closed loop dynamics about the desired maneuver, it is helpful to write the dynamics in a maneuver adapted, *transverse* coordinate system,

$$\begin{aligned} x_p &= \bar{x}_p(v) + z_p \\ x_c &= \bar{x}_c(v) + z_c \\ x_a &= \bar{x}_a + z_a \end{aligned}$$

with transverse coordinates (z_p, z_c, z_a) about the maneuver $(v, \bar{x}_p(v), \bar{x}_c(v), \bar{x}_a), v \geq 0$.

First, using (3), note that the evolution of v simplifies from its nonlinear form (1) to

$$\dot{v} = a_d + c_p^T z_p \,.$$

Next,

$$\begin{aligned} \dot{z}_p &= \dot{x}_p - \bar{x}_p'(v)\, \dot{v} \\ &= A_p(\bar{x}_p(v) + z_p) + b_p c_c^T (\bar{x}_c(v) + z_c) - b_p d_c c_a^T (\bar{x}_a + z_a) \\ &\qquad + b_p d_c (a_d - g) - \bar{x}_p'(v)\, (a_d + c_p^T z_p) \\ &= A_p z_p + b_p c_c^T z_c - b_p d_c c_a^T z_a - \bar{x}_p'(v) c_p^T z_p \end{aligned}$$

where we have made use of (4) and (6). Using (5), we see that

$$\dot{z}_c = A_c z_c - b_c c_a^T z_a - \bar{x}_c'(v) c_p^T z_p$$

and finally, using (3) and (7),

$$\dot{z}_a = A_a z_a + b_a c_p^T z_p \,.$$

Collecting these results, we obtain

$$\dot{v} \;=\; a_d + c_p^T z_p \tag{8}$$

$$\begin{bmatrix} \dot{z}_p \\ \dot{z}_c \\ \dot{z}_a \end{bmatrix} = \begin{bmatrix} A_p - \vec{x}_p'(v) c_p^T & b_p c_c^T & -b_p d_c c_a^T \\ -\vec{x}_c'(v) c_p^T & A_c & -b_c c_a^T \\ b_a c_p^T & 0 & A_a \end{bmatrix} \begin{bmatrix} z_p \\ z_c \\ z_a \end{bmatrix} \tag{9}$$

so that the dynamics is nearly linear, with only the "system matrix" depending on the tangential state v. Note that (8), (9) is *nonlinear*, containing in particular $v\, c_p^T z_p$, so that the above linear stability analysis will not be sufficient to conclude reasonable system behavior.

To simplify the maneuver regulation analysis, it is helpful to do a coordinate change in the *tangential* direction so that the tangential state evolves at the same rate as time when on the maneuver. Defining $\theta = v/a_d$, we obtain

$$\dot{\theta} \;=\; 1 + (1/a_d)\, c_p^T z_p \tag{10}$$

$$\begin{bmatrix} \dot{z}_p \\ \dot{z}_c \\ \dot{z}_a \end{bmatrix} = \begin{bmatrix} A_p - \vec{x}_p'(a_d\theta) c_p^T & b_p c_c^T & -b_p d_c c_a^T \\ -\vec{x}_c'(a_d\theta) c_p^T & A_c & -b_c c_a^T \\ b_a c_p^T & 0 & A_a \end{bmatrix} \begin{bmatrix} z_p \\ z_c \\ z_a \end{bmatrix} \tag{11}$$

so that the transverse dynamics depends in an essential manner on the particular maneuver $\bar{x}(\cdot)$ through its derivative $\vec{x}'(\cdot)$.

Since $\bar{x}(v)$ is a quadratic polynomial, its derivative $\vec{x}'(v)$ is affine in $v = a_d\theta$. Making use of the calculations defining $\tilde{x}(\cdot)$ and $\bar{x}(\cdot)$ above, one may show that

$$\vec{x}_p'(a_d\theta) = -2ba_d\,[(A_p^{-2}b_p + c_p^T A_p^{-2} b_p\, A_p^{-1} b_p) + A_p^{-1} b_p\, \theta]$$

$$\vec{x}_c'(a_d\,\theta) = \quad 2ba_d \begin{bmatrix} (c_p^T A_p^{-2} b_p - k_R/k_Q)/k_Q + \theta/k_Q \\ 1/k_Q \\ 0 \end{bmatrix}$$

so that

$$\begin{aligned} \frac{\vec{x}'(a_d\,\theta)}{2ba_d} &= \begin{bmatrix} -(A_p^{-2}b_p + c_p^T A_p^{-2} b_p\, A_p^{-1} b_p) \\ \begin{bmatrix} (c_p^T A_p^{-2} b_p - k_R/k_Q)/k_Q \\ 1/k_Q \\ 0 \end{bmatrix} \\ 0 \end{bmatrix} + \begin{bmatrix} -A_p^{-1} b_p \\ \begin{bmatrix} 1/k_Q \\ 0 \end{bmatrix} \\ 0 \end{bmatrix} \theta \\ &=: \bar{x}_1 + \bar{x}_2\,\theta \end{aligned}$$

defining the vectors $\bar{x}_1$ and $\bar{x}_2$ which are independent of the desired acceleration a_d and drag parameter b, depending only on the (realization) parameters of the propeller/servo system and the PIRQ control system gains.

Using $\rho^T = (z_p^T, z_c^T, z_a^T)$ and $\bar{c}^T = (c_p^T, 0, 0)$, the maneuver dynamics are thus given by

$$\dot{\theta} = 1 + (1/a_d)\, \bar{c}^T \rho \tag{12}$$

$$\begin{aligned} \dot{\rho} &= (\bar{A} - 2ba_d\, \bar{x}_1 \bar{c}^T - 2ba_d\, \bar{x}_2\, \theta\, \bar{c}^T)\, \rho \\ &=: A(\theta)\, \rho \end{aligned} \tag{13}$$

where $\bar{A}$ is the system matrix from (2) that characterizes the dynamics of the linear feedback system in Figure 4. Recall that the accelerating descent occurs within a finite amount of time, space, and velocity due to such constraints. The usual notions of asymptotic stability are not so useful in this case. We may, however, require that the maneuver $\rho = 0$ be *exponentially attractive* in the sense that $\|\rho(t)\| \leq Me^{-\alpha t}\|\rho(0)\|$, for some $\alpha > 0$, $M < \infty$, until we terminate the maneuver and recover from the *dive* (for velocity or altitude requirements, for instance).

The dynamics (12), (13) is depicted in Figure 6, showing special features of its feedback structure. Given that we can

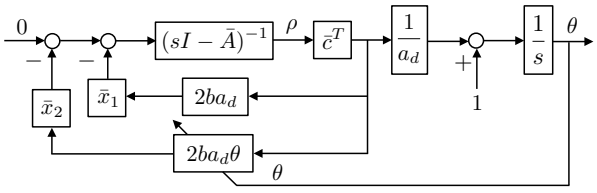

Fig. 6. Transverse dynamics with θ dependent feedback

fly only over finite range of θ (or v), it makes sense to consider the θ dependent feedback gain as a sector bounded time-varying nonlinear feedback. It is thus natural to consider an analysis based on the circle criterion [7]:

Theorem 2 (Circle Criterion): Let $G(s)$ be stable and such that its Nyquist plot is to the right of $-1/\beta$, $\beta > 0$, i.e., Re $G(j\omega) \geq -1/\beta$ for all $\omega \in \mathbb{R}$. Then, the system with time-varying nonlinear (negative) feedback belonging to the sector $[0, \beta - \varepsilon]$, $\varepsilon > 0$ will be absolutely stable.

We have the following result.

Theorem 3: Suppose that the PIRQ controller parameters have been chosen so that $\bar{A}$ is Hurwitz. Then, for each $a_d > 0$ in the open interval such that $\bar{A} - 2ba_d \bar{x}_1 \bar{c}^T$ is Hurwitz, there is a $\bar{v} > 0$ and symmetric matrices $P, Q > 0$ such that

$$A(\theta)^T P + PA(\theta) + Q \leq 0 \tag{14}$$

for all $\theta \in [0, \bar{v}/a_d]$. Each such a_d maneuver is thus exponentially attractive on $\theta \in [0, \bar{v}/a_d]$.

Proof: Let a_d be such that $\bar{A} - 2ba_d \bar{x}_1 \bar{c}^T$ is Hurwitz and let $\beta > 0$ be such that Re $\{2ba_d \bar{c}^T (j\omega I - \bar{A} + 2ba_d \bar{x}_1 \bar{c}^T)^{-1} \bar{x}_2\} > -1/\beta$ for all $\omega \in \mathbb{R}$. By the circle criterion, it is then clear that linear parameter-varying system, with *parameter* θ,

$$\dot{\rho} = A(\theta(t))\rho$$

is absolutely stable for any $\theta(\cdot)$ curve with $\theta(t) \in [0, \beta]$ for all $t \geq 0$. The desired P and Q matrices may be constructed using the Kalman-Yakubovich-Popov lemma showing that the transverse dynamics is in fact quadratically stable. ■

Given $a_d > 0$ and $\bar{v}$ with corresponding P, Q, it is now easy to see that the a_d maneuver is exponentially attractive on $\theta \in [0, \bar{v}/a_d]$. Indeed, differentiating the *transverse* Lyapunov function [3]

$$V(\theta, \rho) = \rho^T P \rho$$

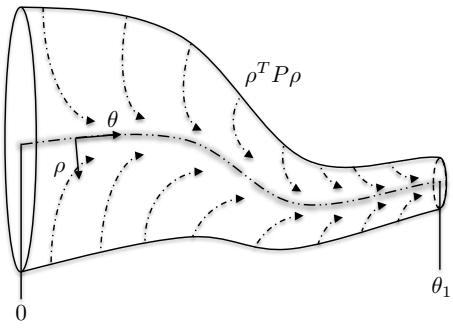

Fig. 7. A transverse Lyapunov function for maneuver *stability*

along the dynamics (12), (13) gives

$$\dot{V}(\theta,\rho) = \rho^T (A(\theta)^T P + P A(\theta))\rho$$
$$\leq -\rho^T Q \rho < 0$$

for $\theta \in [0, \bar{v}/a_d]$ showing that $\rho = 0$ is exponentially attractive. The matrices P and Q can be used in the usual manner to provide the exponential estimates M and α above. This attractiveness property is illustrated in Figure 7.

Example Analysis

For the sake of illustrating the key features described above, we work through the details with specific models for the propeller/servo and accelerometer systems. Using experimental ID, the propeller/servo system is modeled as

$$G_p(s) = \frac{1250}{s^2 + 56.25s + 1250}$$

with state space realization

$$\left[\begin{array}{c|c} A_p & b_p \\ \hline c_p^T & d_p \end{array}\right] = \left[\begin{array}{cc|c} -56.25 & -39.0625 & 1 \\ 32.00 & 0 & 0 \\ \hline 0 & 39.0625 & 0 \end{array}\right]$$

and the accelerometer system is modeled as

$$G_a(s) = \frac{2.878e04}{s^2 + 84.82s + 2.878e04}.$$

with state space realization

$$\left[\begin{array}{c|c} A_a & b_a \\ \hline c_a^T & d_a \end{array}\right] = \left[\begin{array}{cc|c} -84.82 & -224.84 & 1 \\ 128.00 & 0 & 0 \\ \hline 0 & 224.84 & 0 \end{array}\right].$$

The drag parameter is taken to be $b = 0.06775$. The stabilizing triple integrator controller was taken to be

$$C(s) = \frac{0.4s^3 + 6.4s^2 + 30.4s + 38.4}{s^3}$$

with the state space realization indicated above.

Choosing $a_d = 9.807$ $(1\,g)$ and examining the Nyquist plot of the appropriate circle criterion transfer function, shown in figure 8, we find that $\beta = 28.5$ which leads to a maximum velocity of $\bar{v} = 279.6\,m/s$, very fast compared to an expected maximum of 20 or 30 m/s for our vertical flight test platform. This means that, using the chosen PIRQ controller, the invariant zero g maneuver from $v = 0$ to about $280\,m/s$ will be exponentially attractive.

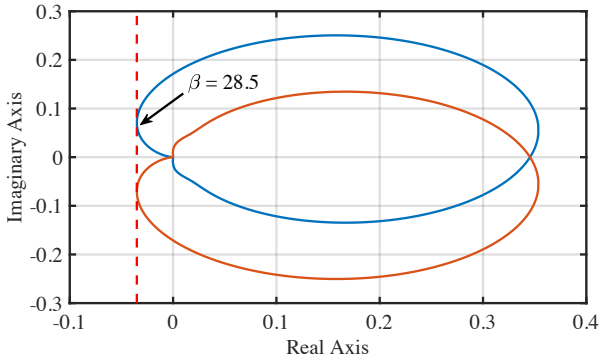

Fig. 8. Circle criterion Nyquist plot

Noting that $A(\theta)$, $\theta \in [0, \theta_1]$, is a matrix polytope, we see that stability certifying matrices P and Q may be found using convex optimization. Indeed, we can use a maximum desired acceleration $\bar{a}_d$ and a maximum velocity $\bar{v}$ to cover a full range of accelerations a_d and corresponding $\bar{\theta} = \bar{v}/a_d$. In that case, we use the convex hull of the four matrices, $\bar{A}$, $\bar{A} - 2b\bar{a}_d \bar{x}_1 \bar{c}^T$, $\bar{A} - 2b\bar{v}\bar{x}_2\bar{c}^T$, and $\bar{A} - 2b\bar{a}_d\bar{x}_1\bar{c}^T - 2b\bar{v}\bar{x}_2\bar{c}^T$. Taking $\bar{a}_d = 9.807$ and $\bar{v} = 30$, we found, using YALMIP [8], that the positive definite, symmetric matrices

$$P = \begin{bmatrix} 4.23 & * & * & * & * & * & * \\ 4.05 & 12.83 & * & * & * & * & * \\ -0.974 & -4.31 & 31.7 & * & * & * & * \\ -1.39 & -4.86 & 21.1 & 21.0 & * & * & * \\ -0.650 & -1.28 & 2.37 & 2.20 & 1.37 & * & * \\ -0.127 & 1.10 & -2.86 & -2.50 & -1.18 & 22.9 & * \\ -2.70 & -5.40 & -0.649 & -1.14 & -0.308 & 5.53 & 42.8 \end{bmatrix}$$

$$Q = \begin{bmatrix} 122 & * & * & * & * & * & * \\ -9.71 & 27.6 & * & * & * & * & * \\ -49.9 & 0.857 & 23.16 & * & * & * & * \\ -33.1 & -3.98 & 14.8 & 13.1 & * & * & * \\ -12.0 & 2.61 & 5.24 & 2.35 & 2.81 & * & * \\ 282 & -115 & -143 & -54.2 & -54.0 & 2270 & * \\ 215 & -10.2 & -79.4 & -96.6 & 2.69 & -127 & 1660 \end{bmatrix}$$

satisfy (14) thereby ensuring that our maneuver is exponentially attractive.

Experimental Demonstration

In addition to theoretical and simulation results, the performance of the PIRQ controller for the regulation of constant acceleration flight has been demonstrated experimentally using the variable pitch multi-rotor shown in figure 9.

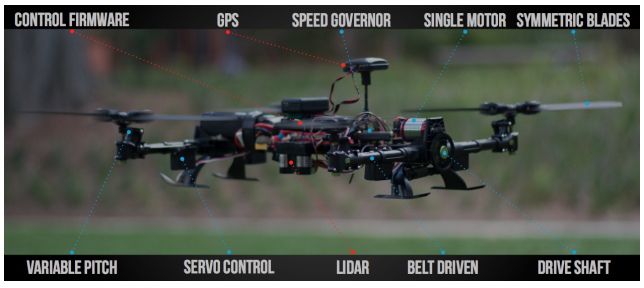

Fig. 9. Experimental Platform - Modified Assault Reaper 500®

The single-motor configuration operates at constant rotor speed and contains four independent pitch actuators resulting in a responsive system with approximately five

times the control bandwidth of a fixed-pitch multi-rotor [9]. The configuration was selected for its ability to produce positive and negative thrust through collective deflections on the actuators while decoupling attitude control authority from thrust required through small independent deviations on blade-pitch.

The flight test demonstrated fully autonomous reduced-gravity parabolic flight, where tracking of 0.378 $G's$ was achieved for a period of approximately 1.5 sec with tolerances of $\pm 0.1G$, a mean within 0.6% from the desired G value and a RMSE of 0.0426 G. The vertical flight-profile is illustrated by Figure 10, where each color represents the active state of the maneuver-governing automata described in [1] and built on the work by [10].

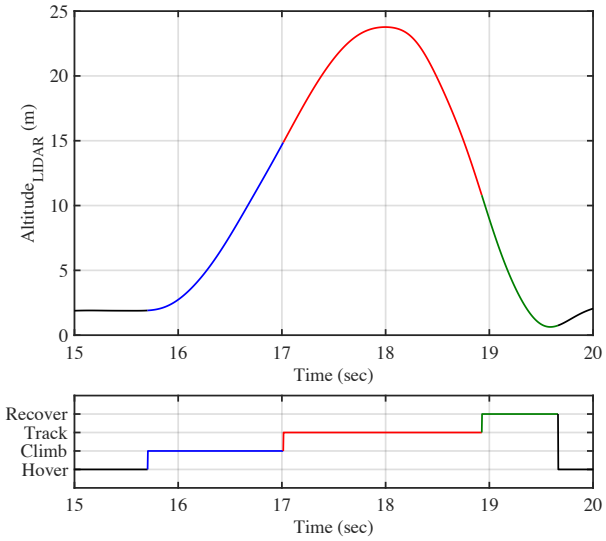

Fig. 10. Autonomous Vertical Maneuver and Automata States. Access Video Through URL: https://youtu.be/-sSCuPzgb3g

Figure 11 illustrates the transients of the raw accelerometer data normalized by $g_0 = -9.807 m/s^2$, the vehicle's altitude, velocity and available collective, for the tracking portion of the autonomous vertical-flight reduced-gravity maneuver.

CONCLUSION

Design and analysis for the novel triple integral PIRQ controller was developed to provide maneuver regulation of a flight vehicle executing a vertical fall with constant acceleration. An internal model principle approach was taken to provide regulation against the quadratic aerodynamic disturbance. While this linear approach seemed effective, the overall system is nonlinear and hence required further analysis. Therefore, a maneuver regulation approach was taken to show that the transverse dynamics were made exponentially attractive. This work has validated the proposed PIRQ controller both theoretically, employing the circle criterion, and experimentally on a flight test vehicle.

REFERENCES

[1] J.-P. Afman, E. Feron, and J. Hauser, "Triple-integral control for reduced-g atmospheric flight," in *American Control Conference*, 2018.

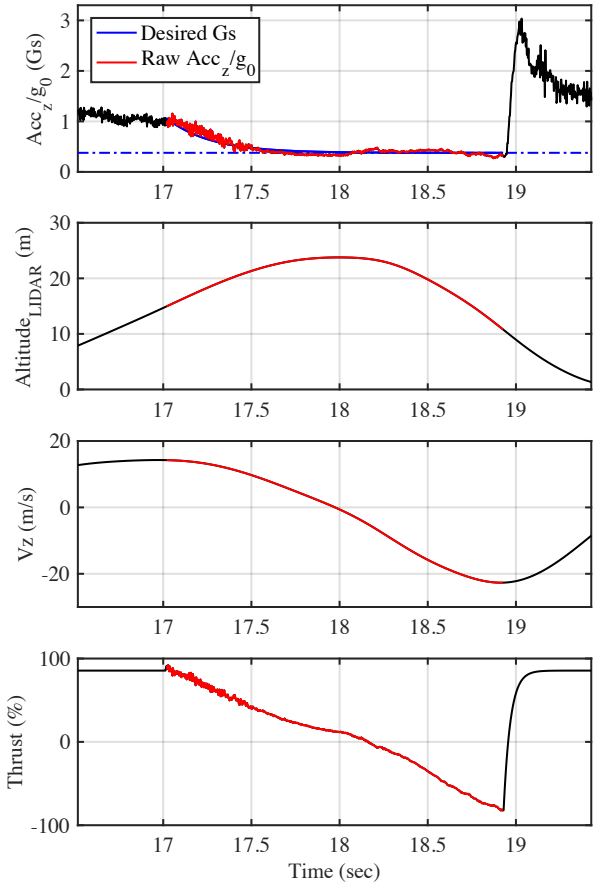

Fig. 11. Martian 0.378 G Maneuver States

[2] J.-P. Afman, J. Franklin, M. L. Mote, T. Gurriet, and E. Feron, "On the design and optimization of an autonomous microgravity enabling aerial robot," *arXiv preprint arXiv:1611.07650*, 2016.

[3] J. Hauser and C. C. Chung, "Converse lyapunov functions for exponentially stable periodic orbits," *Systems & Control Letters*, vol. 23, no. 1, pp. 27–34, 1994.

[4] C. C. Chung and J. Hauser, "Nonlinear control of a swinging pendulum," *automatica*, vol. 31, no. 6, pp. 851–862, 1995.

[5] J. Hauser and R. Hindman, "Maneuver regulation from trajectory tracking: Feedback linearizable systems," *IFAC Proceedings Volumes*, vol. 28, no. 14, pp. 595–600, 1995.

[6] A. Saccon, J. Hauser, and A. Beghi, "A virtual rider for motorcycles: Maneuver regulation of a multi-body vehicle model," *IEEE Transactions on Control Systems Technology*, vol. 21, no. 2, pp. 332–346, 2013.

[7] M. Vidyasagar, *Nonlinear systems analysis*. Prentice Hall, 1978.

[8] J. Lofberg, "Yalmip: A toolbox for modeling and optimization in matlab," in *Computer Aided Control Systems Design, 2004 IEEE International Symposium on*. IEEE, 2004, pp. 284–289.

[9] M. Cutler, N.-K. Ure, B. Michini, and J. How, "Comparison of fixed and variable pitch actuators for agile quadrotors," in *AIAA Guidance, Navigation, and Control Conference*, 2011, p. 6406.

[10] V. Gavrilets, E. Frazzoli, B. Mettler, M. Piedmonte, and E. Feron, "Aggressive maneuvering of small autonomous helicopters: A human-centered approach," *The International Journal of Robotics Research*, vol. 20, no. 10, pp. 795–807, 2001.